

Examples of homology 3-spheres whose Chern-Simons function is not Morse-Bott

Hans U. Boden, Christopher Herald, and Paul Kirk

ABSTRACT. We construct homology 3-spheres for which the (unperturbed) $SU(2)$ Chern-Simons function is not Morse-Bott. In one example, there is a degenerate isolated critical point. In another, a path component of the critical set is not homeomorphic to a manifold. The examples are $+1$ Dehn surgeries on connected sums of torus knots.

1. Introduction

The purpose of this article is to address a question raised by D. Ruberman¹, namely, whether there exist examples of *homology 3-spheres* M for which the $SU(2)$ Chern-Simons function

$$c_M : \mathcal{B}^* \rightarrow \mathbb{R}/\mathbb{Z},$$

a circle-valued function on the space of gauge equivalence classes of irreducible $SU(2)$ connections, fails to be Morse-Bott. We construct an example of a homology 3-sphere whose Chern-Simons function has a degenerate isolated critical point, as well as one for which the critical set of the Chern-Simons function has a path component not homeomorphic to a manifold. It is known that there are Seifert-fibered homology spheres for which the $SU(3)$ Chern-Simons function is not Morse-Bott [BHK05].

As is well known, holonomy identifies the critical set of c_M with the irreducible character variety (a real semi-algebraic set):

$$\chi^*(M) = \text{Hom}(\pi_1(M), SU(2)) \setminus \{\theta\}/\text{conjugation},$$

where θ denotes the trivial homomorphism. For any homomorphism $\rho : \pi_1(M) \rightarrow SU(2)$ (henceforth called a representation), the cohomology group $H^1(M; su(2)_{\text{ad } \rho})$ is called the *Zariski tangent space* of $\chi(M)$ at ρ . Since M is a homology 3-sphere, the conjugacy class $[\theta]$ of θ is isolated in the character variety; it follows that $\chi^*(M)$ is compact [AM90]. The Hodge theorem identifies the kernel of the Hessian of c_M at ρ with the Zariski tangent space of $\chi(M)$ at ρ (e.g., see [Tau90]). The function c_M is Morse if all its critical points are non-degenerate; i.e., the Zariski tangent space is trivial at each critical point. It is widely known that if M is a connected sum of nontrivial homology spheres, c_M is not

2020 *Mathematics Subject Classification.* Primary 57K18, 57K31, 57R58; Secondary 81T13.

Key words and phrases. Chern-Simons function, flat moduli space.

HUB was supported by an NSERC Discovery Grant. CH was supported by a Simons Collaboration Grant for Mathematicians. PK is thankful to MPIM in Bonn for support.

¹Private communication.

Morse because π_1 is a nontrivial free product; there are gluing parameters (also known as bending parameters), related to conjugating a representation of one factor but not the other.

The Chern-Simons function c_M is called Morse-Bott if and only if every path component of the critical set is a smooth manifold, and for each $[\rho] \in \chi^*(M)$ the dimension of the Zariski tangent space of $\chi(M)$ at $[\rho]$ equals the dimension of the path component containing $[\rho]$.

Fintushel-Stern [FS90] showed that if M is a Seifert-fibered homology 3-sphere, then c_M is Morse-Bott. Given two homology spheres M_1, M_2 such that c_{M_i} is Morse-Bott for $i = 1, 2$, the connected sum $M_1 \# M_2$ also has a Morse-Bott Chern-Simons function. In fact, given path components $C_1 \subset \chi^*(M_1)$ and $C_2 \subset \chi^*(M_2)$, there are three associated components in $\chi^*(M_1 \# M_2)$, diffeomorphic to $C_1 \times [\theta_2]$, $[\theta_1] \times C_2$, and $C_1 \times (SU(2)/\{\pm 1\}) \times C_2 \subset \chi^*(M_1 \# M_2)$. The latter is obtained by pairing each ρ_1 representing an equivalence class in C_1 with all $SU(2)$ conjugates of a ρ_2 representing a class in C_2 .

Given relatively prime integers p, q , let $T_{p,q}$ denote the (p, q) torus knot. Consider the knot complements:

$$X = S^3 \setminus \text{nbd}(T_{3,5}), \quad Y = S^3 \setminus \text{nbd}(T_{2,7}), \quad \text{and} \quad Z = S^3 \setminus \text{nbd}(T_{-2,7} \# T_{-2,7}).$$

On a 2-torus T^2 with specified meridian μ and longitude λ , define $h: T^2 \rightarrow T^2$ to be an (orientation-reversing) homeomorphism inducing the map

$$(1) \quad h_*: \mu \mapsto \mu, \quad \lambda \mapsto -\mu - \lambda$$

on the fundamental group. Equip the boundary ∂X with its natural oriented meridian-longitude pair μ_X, λ_X , and similarly μ_Y, λ_Y for Y and μ_Z, λ_Z for Z . Define

$$\Sigma_1 = X \cup_h Y \quad \text{and} \quad \Sigma_2 = X \cup_h Z.$$

It is immediate from the fact that X, Y, Z are all homology solid tori with H_1 generated by the meridians, and with the longitudes trivial in H_1 , that Σ_1, Σ_2 are homology spheres.

THEOREM A.

- (1) *There exists an isolated point in $\chi^*(\Sigma_1)$ with 2-dimensional Zariski tangent space.*
- (2) *There exists a component of $\chi^*(\Sigma_2)$ which is not homeomorphic to a manifold.*

COROLLARY B. *The critical set of c_{Σ_1} contains an isolated point at which the Hessian has a 2-dimensional kernel. The critical set of c_{Σ_2} is not homeomorphic to a manifold.*

Thus c_{Σ_1} and c_{Σ_2} are most decidedly not Morse-Bott. Taking connected sums of these with themselves and with other homology 3-spheres provides many more complicated examples.

We note that results of Kapovich and Millson [KM17] imply that arbitrarily bad singularities, including isolated points with nonzero Zariski tangent space and non-manifold path components, occur in $SU(2)$ character varieties of 3-manifolds. It is an open question whether their universality results hold for homology 3-spheres (see, e.g., [KM17, Question 8.2]).

2. Character varieties of X and Y and their image in the character variety of the separating torus

For any path-connected space A , let

$$\chi(A) = \text{Hom}(\pi_1(A), SU(2))/_{\text{conjugation}}$$

denote its character variety. Its points are conjugacy classes, denoted $[\rho: \pi_1(A) \rightarrow SU(2)]$, or simply $[\rho]$. A representation $\rho: \pi_1(A) \rightarrow SU(2)$ is called *central*, *(non-central) abelian*, or *irreducible*, depending on whether the stabilizer of ρ under conjugation by $SU(2)$ is isomorphic to $\{\pm 1\}$, $U(1)$ or $SU(2)$.

When T^2 is the 2-dimensional torus with a fixed set of generators $\mu, \lambda \in \pi_1(T^2)$, $\chi(T^2)$ is homeomorphic to a 2-sphere (usually called the pillowcase), and there is a branched covering

$$(2) \quad \mathbb{R}^2 \rightarrow \chi(T^2), \quad (x, y) \mapsto [\mu \mapsto e^{xi}, \lambda \mapsto e^{yi}]$$

which can be seen as the composite of the projection $\mathbb{R}^2 \rightarrow \mathbb{R}^2/(2\pi\mathbb{Z})^2$ and the orbit map of the central involution induced by $(x, y) \mapsto (-x, -y)$. Call a curve in $\chi(T^2)$ a *line segment* if it is the image of a line segment in \mathbb{R}^2 . Since the slope of a line is preserved by both translations by $(2\pi\mathbb{Z})^2$ and reflections through the origin, line segments in $\chi(T^2)$ have well-defined slope.

For any knot K , $\chi(S^3 \setminus \text{nbd}(K))$ contains an arc of (conjugacy classes of) abelian representations with central endpoints, mapping to the image of the x axis (i.e., with slope zero) in $\chi(T^2)$. We parameterize this arc with a path of representations $\mu \mapsto e^{ai}, \lambda \mapsto 1$, $a \in [0, \pi]$, where μ, λ are a meridian, longitude pair.

Klassen [Kla91] explicitly identified the $SU(2)$ character varieties of torus knot complements. From his description of families of homomorphisms parameterizing the path components of $\chi^*(S^3 \setminus \text{nbd}(T_{p,q}))$, one can readily restrict to a meridian/longitude which generate $\pi_1(T^2)$ to identify the image of the restriction map

$$i^*: \chi(S^3 \setminus \text{nbd}(T_{p,q})) \rightarrow \chi(T^2)$$

induced by the inclusion $i: T^2 = \partial(S^3 \setminus \text{nbd}(T_{p,q})) \rightarrow S^3 \setminus \text{nbd}(T_{p,q})$. Along with the abelian arc, $\chi(S^3 \setminus \text{nbd}(T_{p,q}))$ consists a collection of arcs of conjugacy classes of irreducible representations, mapping to $\chi(T^2)$ as line segments of slope $-pq$, with ends limiting to certain points on the abelian arc. The details in the case of $T_{3,5}$ are summarized in [HK14]. For the purposes of this article, we require only the following part of this calculation for $T_{3,5}$, $T_{2,7}$, and $T_{-2,7}$.

PROPOSITION 1 (Klassen [Kla91]). *There is a path component of $\chi^*(S^3 \setminus \text{nbd}(T_{3,5}))$ which is an arc mapping onto a line segment in $\chi(T^2)$ of slope -15 , $r \in (\frac{\pi}{15}, \frac{11\pi}{15}) \mapsto (r, -15r)$, with ends limiting to the points $a = \frac{\pi}{15}$ and $a = \frac{11\pi}{15}$ on the abelian arc. Similarly, there is path component of $\chi^*(S^3 \setminus \text{nbd}(T_{\pm 2,7}))$ mapping onto a line segment in $\chi(T^2)$ of slope ∓ 14 , $r \in (\frac{\pi}{14}, \frac{13\pi}{14}) \mapsto (r, \mp 14r)$, with ends limiting to the points $a = \frac{\pi}{14}$ and $a = \frac{13\pi}{14}$ on the abelian arc.*

At each interior point on these irreducible arcs, the Zariski tangent space is 1-dimensional. For the (abelian) endpoints of either irreducible arc, the Zariski tangent space is 3-dimensional and the linearization of the restriction map to $\chi(T^2)$ has rank one, with horizontal image.

Figure 1 and Figure 2 illustrate neighborhoods of the left ends of the irreducible arcs described in the theorem and (lifts to \mathbb{R}^2 of) their images under restriction to the character variety of the boundary torus. In both cases, the neighborhoods embed into the pillowcase.

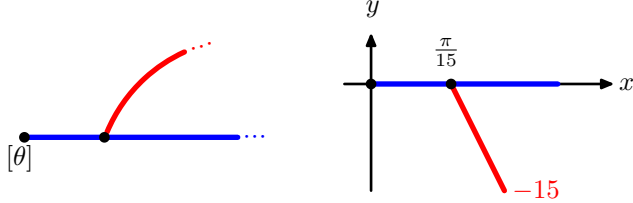


FIGURE 1. Local picture of $\chi(X) = \chi(S^3 \setminus \text{nbhd}(T_{3,5}))$ near $[\theta]$ (on left) and its image under $i_X^* : \chi(X) \rightarrow \chi(\partial X)$ (on right)

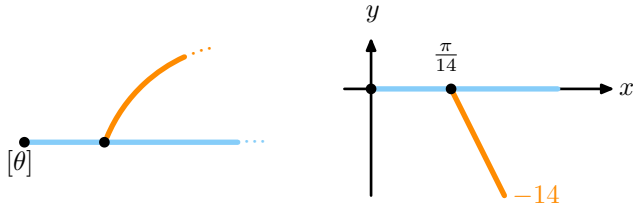


FIGURE 2. Local picture of $\chi(Y) = \chi(S^3 \setminus \text{nbhd}(T_{2,7}))$ near $[\theta]$ (on left) and its image under $i_Y^* : \chi(Y) \rightarrow \chi(\partial Y)$ (on right)

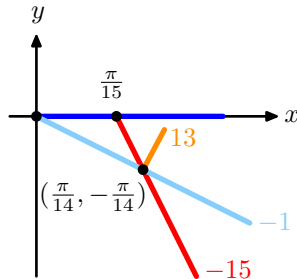


FIGURE 3. The images $i_X^* (\chi(X))$ and $h^* \circ i_Y^* (\chi(Y))$ near $[\theta]$ in $\chi(\partial X)$

3. Proof of Theorem A

3.1. Proof of part (1). The homeomorphism h of Equation (1) induces a map $h^* : \chi(\partial Y) \rightarrow \chi(\partial X)$ which lifts to the linear map

$$h^* = \begin{pmatrix} 1 & 0 \\ -1 & -1 \end{pmatrix}$$

on \mathbb{R}^2 , using (2). Figure 3 illustrates the line segments which make up the images under the local embeddings i_X^* and $h^* \circ i_Y^*$ of the portions of $\chi(X)$ and $\chi(Y)$ in Figures 1 and 2.

Consider the fiber product

$$F := \{([\rho_X], [\rho_Y]) \mid i_X^*(\rho_X) = h^* \circ i_Y^*(\rho_Y)\} \subset \chi(X) \times \chi(Y).$$

The restriction map $\chi(\Sigma_1) \rightarrow \chi(X) \times \chi(Y)$ has image F and fiber over $([\rho_X], [\rho_Y])$ (known as the space of *gluing parameters*) homeomorphic to the double coset space

$$(3) \quad \text{Stab}_{\rho_X} \setminus \text{Stab}_{\rho_{\partial X}} / \text{Stab}_{\rho_Y}$$

(see, e.g., [HHK14]).

From the subsets of $i_X^*(\chi(X))$, $h^*(i_Y^*(\chi(Y)))$ that we have identified and sketched in Figure 3, it is clear that there are two isolated points of intersection. Specifically, $([\theta_X], [\theta_Y])$ maps to the origin in $\chi(\partial X) = \mathbb{R}^2 / \sim$, and a pair $([\rho_X], [\rho_Y])$ which maps to $(\frac{\pi}{14}, -\frac{\pi}{14})$. Moreover, ρ_X has non-abelian image and ρ_Y has abelian but non-central image.

For this second pair, $\text{Stab}_{\rho_{\partial X}} = U(1) = \text{Stab}_{\rho_Y}$, since the representations ρ_Y and $\rho_{\partial X}$ are abelian non-central. Hence the pair $([\rho_X], [\rho_Y])$ mapping to $(\frac{\pi}{14}, -\frac{\pi}{14})$ corresponds to an *isolated point* of (the real semi-algebraic set) $\chi(\Sigma_1)$.

Consider the Mayer-Vietoris sequence (with local $su(2)$ coefficients)

$$\cdots \xrightarrow{0} H^1(\Sigma_1) \longrightarrow H^1(X) \oplus H^1(Y) \xrightarrow{i_X^* - h^* \circ i_Y^*} H^1(\partial X) \longrightarrow \cdots$$

We have:

- $\dim H^1(X; su(2)_{ad\rho_X}) = 1$ because $[\rho_X]$ is an interior point on the irreducible arc of $\chi(X)$ identified in Proposition 1,
- $\dim H^1(\partial X; su(2)_{ad\rho_{\partial X}}) = 2$ since the restriction $\rho_{\partial X}: \pi_1(\partial X) \rightarrow SU(2)$ is abelian and non-central,
- $\dim H^1(Y; su(2)_{ad\rho_Y}) = 3$ because ρ_Y is the $a = \frac{\pi}{14}$ abelian endpoint of the irreducible arc of $\chi(Y)$ identified in Proposition 1, and
- the image of the irreducible arc in $\chi^*(X)$ and the abelian arc in $h^*(i_Y^*(\chi(Y)))$ have different slopes in $\chi(\partial X)$, namely -15 and -1 , respectively, which shows $i_X^* - h^* \circ i_Y^*$ is surjective.

Thus, the Mayer-Vietoris sequence implies that $\dim H^1(\Sigma_1; su(2)_{ad\rho}) = 2$, completing the proof of the first assertion of Theorem A.

3.2. Proof of part (2). The proof of Part (2) of Theorem A follows a similar strategy to that used to prove Part (1), but we replace Y by $Z = S^3 \setminus nbd(T_{-2,7} \# T_{-2,7})$. The exterior Z of the composite knot $T_{-2,7} \# T_{-2,7}$ may be viewed as the union of the two exteriors

$$Z_1 = Z_2 = S^3 \setminus nbd(T_{-2,7})$$

along an annulus representing a meridian. We begin by describing the relevant subset of $\chi(Z)$ and its image $i_Z^*(\chi(Z)) \subset \chi(\partial Z)$.

The fundamental group $\pi_1(Z)$ is an amalgamated free product of $\pi_1(Z_1)$ and $\pi_1(Z_2)$, where particular meridians on each of the two knot complements are identified. For any representations $\rho_i: \pi_1(Z_i) \rightarrow SU(2)$, $i = 1, 2$, which agree on the identified meridians, there is a representation of $\pi_1(Z)$ that restricts to ρ_i on $\pi_1(Z_i)$. The longitude for the composite knot is the product of the longitudes for Z_1 and Z_2 so, roughly speaking, the longitudinal coordinates in the pillowcase pictures for Z_1, Z_2 add.

The fiber product/gluing parameter results above (this time with restrictions to the annulus instead of to ∂X) demonstrate that abelian arcs and the irreducible arcs in $\chi(Z_i)$, $i = 1, 2$, described in Proposition 1 give rise to the following subsets of $\chi(Z)$:

- (i) the abelian arc in $\chi(Z)$,

- (ii) two *half-abelian arcs*, namely an abelian/irreducible arc and an irreducible/abelian arc, consisting of representations of $\pi_1(Z)$ that are irreducible on only one of $\pi_1(Z_i)$, and
- (iii) a cylinder of irreducible/irreducible representations with S^1 gluing parameter.

All three components of $\chi(Z)$ described in (ii) and (iii) limit to the abelian points $a = \frac{\pi}{14}, \frac{13\pi}{14}$ on the abelian arc of $\chi(Z)$. Under i_Z^* , the abelian arc maps to the (image in $\chi(\partial Z)$ of) the x axis; the two half abelian arcs in (ii) map to line segments of slope 14, and the cylinder in (iii) maps onto a line segment of slope 28. This is summarized in Figure 4.

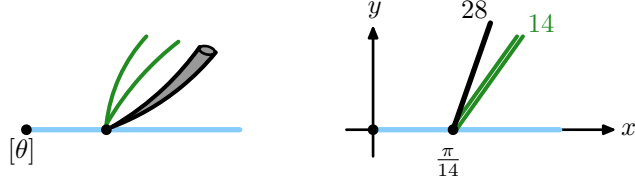


FIGURE 4. Local picture of $\chi(Z) = \chi(S^3 \setminus \text{nbd}(T_{-2,7} \# T_{-2,7}))$ near $[\theta]$ (on left) and its image under $i_Z^*: \chi(Z) \rightarrow \chi(\partial Z)$ (on right)

Under the map $h^*: \chi(\partial Z) \rightarrow \chi(\partial X)$, the origin is fixed (i.e., $h^*([\theta_{\partial Z}]) = [\theta_{\partial X}]$), the abelian arc in $\chi(Z)$ maps to the line segment $y = -x$, the half abelian arcs described above map onto line segments leaving the abelian arc with slope -15 , and the image of the cylinder maps onto a line segment of slope -29 . This is summarized in Figure 5.

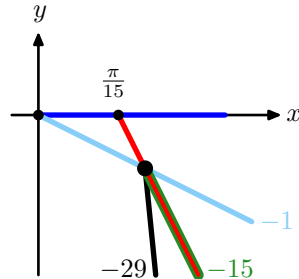


FIGURE 5. The images $i_X^*(\chi(X))$ and $h^* \circ i_Z^*(\chi(Z))$ near $[\theta]$ in $\chi(\partial X)$

In Figure 5, we overlay the images of $i_X^*(\chi(X))$ and $h^*(i_Z^*(\chi(Z)))$ in the same picture, so that we can apply the same sort of fiber product/gluing parameter reasoning to $\Sigma_2 = X \cup_h Z$. We begin by noting that the abelian arc of $\chi(Z)$ meets the irreducible arc in $\chi(X)$ drawn in Figure 1 at the point $(\frac{\pi}{14}, -\frac{\pi}{14})$. This intersection corresponds to a point $[\rho_0] \in \chi(\Sigma_2)$ restricting to an irreducible representation of $\pi_1(X)$ and an abelian representation of $\pi_1(Z)$, so there is no gluing parameter. Nearby, however, the intersection includes a line segment emanating down from this point with slope -15 . The preimage of that segment in $\chi(X)$ is the irreducible arc in Figure 1 and the preimage in $\chi(Z)$ is the left ends of the two half-abelian arcs on in Figure 4.

Taking gluing parameters into account, $[\rho_0]$ has a neighborhood in $\chi(\Sigma_2)$ which is a cone on two disjoint circles, so the path component containing $[\rho_0]$ is not a manifold. This proves the second assertion of Theorem A. \square

4. Further discussion and other examples

We note the following fact about the homology 3-spheres Σ_1, Σ_2 .

PROPOSITION 2. *The homology 3-sphere Σ_1 is diffeomorphic to +1 Dehn surgery on $T_{3,5} \# T_{2,7}$, and Σ_2 is diffeomorphic to +1 Dehn surgery on $T_{3,5} \# T_{-2,7} \# T_{-2,7}$. They are both graph manifolds.*

More lengthy calculations using similar techniques allow the analysis of the full character varieties of Σ_1 and Σ_2 , as well as more complicated constructions involving additional torus knot complements. We highlight a few related results without proof for the interested reader.

PROPOSITION 3. *The irreducible character variety $\chi^*(\Sigma_1)$ consists of 22 isolated points with trivial Zariski tangent space, six isolated points with 2-dimensional Zariski tangent space like the one we described in detail, and a collection of Morse-Bott circle components.*

While we have focused in this paper on the unperturbed Chern-Simons function, the effect of a small (carefully selected) holonomy perturbations on $\chi(\Sigma_1)$ is also reasonably straightforward to understand. A simple holonomy perturbation in a neighborhood of ∂X can be selected so that $i_X^*(\chi(X))$ undergoes a vertical Hamiltonian flow supported away from the central endpoints on the abelian arc, so that each of the six singular isolated points resolves into a Morse critical point and the Morse-Bott circle components remain (see, for example, [HK18]). Under a further perturbation using a curve that cuts through ∂X to break the symmetry giving rise to the gluing parameters, the Chern-Simons function can be made into a Morse function; the Morse-Bott circles can be seen to each contribute two isolated critical points (contributing zero points, counted algebraically, to the Casson invariant).

For clarity, the figures only show the neighborhood of the left endpoints of the irreducible arcs described in Proposition 1, but the irreducible arc parameterizations in that proposition show that the $T_{\pm 2,7}$ arcs extend further to the right than the irreducible $T_{3,5}$ arc. The following proposition is easily proved by tracking the images of the entire half-abelian arcs (see the last two paragraphs of Section 3.2).

PROPOSITION 4. *The path component of $\chi^*(\Sigma_2)$ containing the singular point $[\rho_0]$ is homeomorphic to a wedge of two 2-spheres.*

PROPOSITION 5. *If one replaces Z with $S^3 \setminus \text{nbd}(3T_{-2,7} \# T_{2,7})$ in the construction of Σ_2 , then the corresponding point at $(\frac{\pi}{14}, -\frac{\pi}{14})$ has a neighborhood that is a cone on the disjoint union of two circles and a 3-torus.*

Finally, we note that the homology spheres Σ_1, Σ_2 can also be decomposed into Heegaard decompositions, giving rise to different fiber product descriptions of the singularities in Theorem A. In this case, the character varieties of the handlebodies are smooth manifolds and the local singular structure in the fiber product for this decomposition is a consequence of these handlebody character varieties intersecting nontransversely in the smooth locus of the character variety of the surface.

References

[AM90] Selman Akbulut and John D. McCarthy, *Casson's invariant for oriented homology 3-spheres*, Mathematical Notes, vol. 36, Princeton University Press, Princeton, NJ, 1990, An exposition. MR 1030042

- [BHK05] Hans U. Boden, Christopher M. Herald, and Paul A. Kirk, *The integer valued $SU(3)$ Casson invariant for Brieskorn spheres*, J. Differential Geom. **71** (2005), no. 1, 23–83. MR 2191768
- [FS90] Ronald Fintushel and Ronald J. Stern, *Instanton homology of Seifert fibred homology three spheres*, Proc. London Math. Soc. (3) **61** (1990), no. 1, 109–137. MR 1051101
- [HHK14] Matthew Hedden, Christopher M. Herald, and Paul Kirk, *The pillowcase and perturbations of traceless representations of knot groups*, Geom. Topol. **18** (2014), no. 1, 211–287. MR 3158776
- [HK18] Christopher M. Herald and Paul Kirk, *Holonomy perturbations and regularity for traceless $SU(2)$ character varieties of tangles*, Quantum Topol. **9** (2018), no. 2, 349–418. MR 3812815
- [Kla91] Eric Paul Klassen, *Representations of knot groups in $SU(2)$* , Trans. Amer. Math. Soc. **326** (1991), no. 2, 795–828. MR 1008696
- [KM17] Michael Kapovich and John J. Millson, *On representation varieties of 3-manifold groups*, Geom. Topol. **21** (2017), no. 4, 1931–1968. MR 3654101
- [Tau90] Clifford Henry Taubes, *Casson’s invariant and gauge theory*, J. Differential Geom. **31** (1990), no. 2, 547–599. MR 1037415

MATHEMATICS AND STATISTICS, McMaster University, Hamilton, ON L8S 4K1, Canada
Email address: `boden@mcmaster.ca`

DEPARTMENT OF MATHEMATICS AND STATISTICS, UNIVERSITY OF NEVADA, RENO, NV 89557
Email address: `herald@unr.edu`

DEPARTMENT OF MATHEMATICS, INDIANA UNIVERSITY, BLOOMINGTON, IN 47405
Email address: `pkirk@indiana.edu`